Bull. Mater. Sci., Vol. 38, No. 5, September 2015, pp. 1329–1332. © Indian Academy of Sciences.

Observation of the nano-effect on the SHG in moderately Cu-doped CdI_2 thin nanocrystals

M I MIAH[1,2]

[1]Department of Physics, University of Chittagong, Chittagong, Chittagong 4331, Bangladesh
[2]Queensland Micro- and Nanotechnology Centre, Griffith University, Nathan, Brisbane, QLD 4111, Australia

MS received 24 December 2014; accepted 2 April 2015

Abstract. Nanocrystals take into account the nano-sized quantum-confined effect, where k-space bulk-like dispersion disappears and discrete excitonic-like nanolevels occur within the forbidden energy gap of the material processes. Nanocrystals of cadmium iodide both un-doped and doped with copper, synthesized and grown by the standard Bridgman method, were analysed by scanning electron microscopy for the investigation of the nano-confined effect on the optical nonlinearity. The second harmonic generation (SHG) of the crystals was measured and studied. The second-order optical susceptibilities in dependences of the size of the nanocrystals and of their copper contents within low levels were calculated. The results showed a clear increase in the SHG with the decrease in the thickness of the nanocrystals. The observed size dependence, however, demonstrates the nano-confined effect or nano-effect on the SHG, where the quantum confinement dominates the material's optical properties. A significant change in the second-order optical response with copper content of the nanocrystals was also observed. The observed results are discussed by exploring the photo-induced electron–phonon anharmonic interaction for the noncentrosymmetry of the nanocrystallite's process.

Keywords. Layered semiconductor; nanocrystals; second harmonic generation; nano-effect.

1. Introduction

In recent times optical nonlinear nanomaterials have been investigated from the point of view of nonlinear quantum processes and their potential in applications such as opto-electronic nanodevices. The second harmonic generation (SHG) in materials is an important technique to study the higher-order nonlinear optical processes.[1] As the technique probes particularly the surface effects of an optical material, it is very useful for nano-sized materials.

The nanometre-sized crystals, or nanocrystals in short, take into account the nano-sized quantum-confined effect or nano-confined effect or nano-effect (quantum confinement dominates the material's electronic and optical properties), where **k**-space bulk-like dispersion disappears and discrete excitonic-like nanolevels occur within the forbidden energy gap of the material processes.[2]

Cadmium iodide (CdI_2) having layered structure and space group C_{6v}^4 is an indirect bandgap semiconductor, which has highly anisotropic chemical bonds. The band structure calculations of the CdI_2 crystals have also shown a large anisotropy[3–5] in the space-charge density distribution causing high anisotropy in the corresponding optical spectra. The anisotropic behaviour of the CdI_2 crystals favours the local noncentrosymmetry.

Multiphoton spectroscopy has, in recent times, been performed in pure CdI_2 single crystals. The results show that CdI_2 processes third-order optical nonlinearities.[6–10] However, Cu-doped CdI_2 crystals were first studied by Kityk *et al*,[11] where they studied magnetic field-induced ferroelectricity and showed that the introduction of Cu-doping in CdI_2 makes the crystal noncentrosymmetric. Subsequent investigations for the systems are also available in the literature.[12–15] Here, in this investigation, we study the size dependence of the SHG in Cu-doped CdI_2 nanoscopic crystals and explore the nano-confinement effect.

2. Experimental

Samples of different thicknesses were taken from nanocrystals of Cu-doped CdI_2, synthesized from the mixture of CdI_2 and cuprous iodide. Structures were monitored using a scanning electron microscope (SEM). Figure 1 shows a typical SEM image of the nanocrystals with size of 5 nm. The optical bandgap (E_g) of the nanocrystals was estimated from an indirect transition. To do that, the absorption spectra for the nanocrystals were measured. A typical spectral distribution of absorption coefficient (α)

(m.miah@griffith.edu.au)

is shown in figure 2. Assuming parabolic bands, the relation between α and E_g for an indirect type of transition is given by

$$\alpha E_\lambda = \frac{a_1(E_\lambda - E_g + E_{ph})^n}{\exp(\Theta_D/T)-1} + \frac{a_2(E_\lambda - E_g - E_{ph})^n}{1-\exp(-\Theta_D/T)}, \quad (1)$$

where $E_\lambda = hc/\lambda$ is the photon energy, λ the wavelength of light, Θ_D the Debye temperature, E_{ph} the phonon energy assisting the indirect transition, a_1 and a_2 are constants and $n = 2$ or 3 depending on whether the transition is allowed (2) or forbidden (3) in quantum mechanical sense. The method of determining E_g was to plot a graph of $(\alpha E_\lambda)^{1/n}$ *vs.* E_λ and look for those values of n which give the best linear fits in the two absorption edge regions.

The SHG experiment was performed at liquid helium temperature by mounting the samples in a temperature-regulated cryostat. We used a Nd : YAG laser, as a fundamental laser for the SHG, which generates ps pulses (average power 15 MW) with a repetition rate of 80 mHz. The output SHG ($\lambda = 530$ nm) and fundamental ($\lambda =$ 1060 nm) signals were spectrally separated by a grating monochromator (F) with a spectral resolution of ~ 5 nm mm^{-1}. Detection of the doubled-frequency output SHG signal was performed by a photomultiplier (PMT) with an electronic boxcar integrator (EBI) for the registration of the output. During evaluation of the time-delayed nonlinear optical response, we measured the light intensities at the fundamental (ω) and doubled frequencies (2ω) with time steps of ~ 50 fs using the EBI in the time-synchronized pump–probe conditions. A schema of the experimental set-up is shown in figure 3.

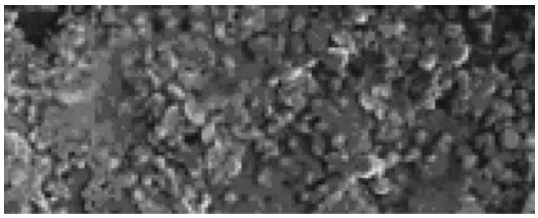

Figure 1. SEM image of typical copper-doped cadmium iodide nanocrystals with size of 5 nm.

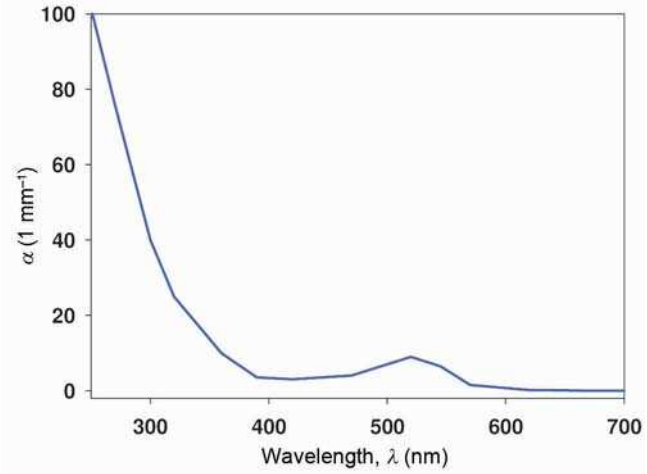

Figure 2. Typical spectral distribution of absorption coefficient of CdI_2–Cu nanocrystals.

3. Results and discussion

The determined value of $E_g = 3.7$ eV, as obtained from the $(\alpha E_\lambda)^{1/2}$ *vs.* E_λ plot, agrees well with those in the literature, obtained experimentally as well as from the band structure calculations for the pure CdI_2.[2–4,7]

Figure 4 shows the SHG signals as a function of pump power density for different thicknesses of the nanocrystals. As can be seen, the SHG increases with the decrease in the thickness (D) of the nanocrystals. The SHG dependence shows a beginning of slight preserve and is increased before reaching a value a little higher than background signal for the thick nanolayers. The SHG for the bulk crystal is zero, or within the background level. However, a significant enhancement in the SHG occurs

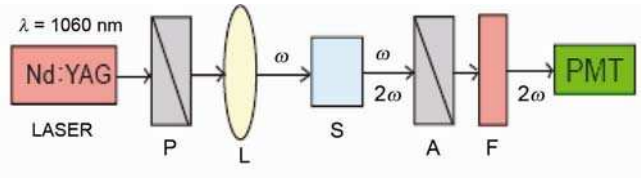

Figure 3. Schema of the experimental set-up for the measurements of the IR-induced SHG.

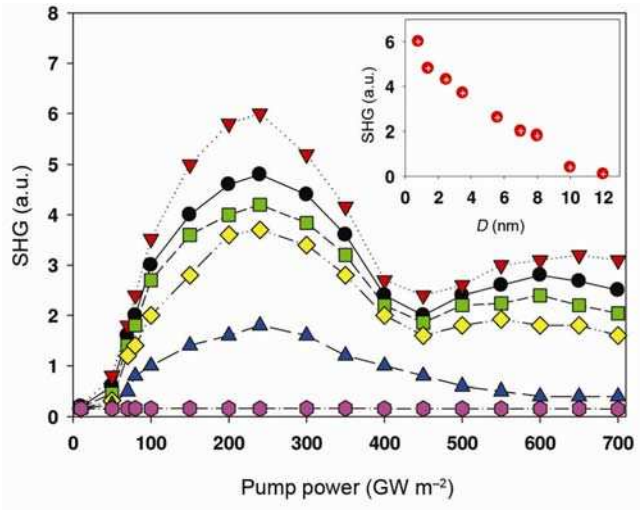

Figure 4. SHG as a function of pump power for various thicknesses of the nanocrystals: (from bottom) bulk (circle), triangle up (8 nm), diamond (3.5 nm), square (2.5 nm), circle (1.4 nm) and triangle down (0.8 nm). Inset shows the dependence of the SHG on the size of the nanocrystals.

for the nanocrystals with thickness lower than 8 nm. The maximum SHG signal as a function of the thickness of the nanocrystals is shown in the inset of figure 4. As seen, the maximum SHG is obtained for the thinnest nanocrystals. However, lowering the thickness of the nanocrystal from 8 nm shows another feature, in which SHG has a weak secondary maximum near 600 kW mm^{-1}. The secondary maximum seems to be shifted slightly in the higher pump power density with the decrease in the thickness of the nanocrystals. The qualitative and quantitative changes that occurred for the thinner nanocrystals correspond to the manifestation of the quantum-confined excitonic levels perpendicularly to the layers. The discrete excitonic-like nanolevels might occur within the forbidden energy gap of the material non-degenerating the bulk-like dispersion in the **k**-space.

The relatively large relaxation time observed in the SHG pulses demonstrates the principal role of long-lived electron–phonon states in the observed effects, as explained within a model of photo-induced electron–phonon anharmonicity,[11,15,16] where the relaxation time for the thin nanolayers should be larger than for the strong localized electron–phonon states due to the nano-size-confined effect.

Nonlinear optical effects are generally described by the optical response of a material medium to an effective electric field E. In the dipole approximation, the polarization of the light field interacting with a medium under high-intensity optical illumination can phenomenologically be expressed as[17]

$$P(\vec{r},t) = \chi_{ij}^{(1)} E_j(\vec{r},t) + \chi_{ijk}^{(2)} E_j E_k(\vec{r},t) + \chi_{ijkl}^{(3)} E_j E_k E_l(\vec{r},t) + \cdots, \quad (2)$$

where $\chi_{ij}^{(1)}$ is the susceptibility tensor of the first order and rank 2. The term $\chi_{ij}^{(1)}$ is responsible for linear optical phenomena such as reflection and refraction of light. The terms $\chi_{ijk}^{(2)}$ and $\chi_{ijkl}^{(3)}$ are responsible for nonlinear optical phenomena and correspond to the second- and third-order optical effects, respectively. Here E_k and E_l are electric field components of the electric field of the electromagnetic wave participating optical illumination.

The generation of optically induced doubled frequency (2ω) second harmonic light is described by the second term in equation (2). The second harmonic polarization of the medium as a function of the frequency (ω) of the fundamental light is given by

$$P_i(2\omega) = \chi_{ijk}^{(2)} E_j(\omega) E_k(\omega). \quad (3)$$

The third rank and second-order tensor $\chi_{ijk}^{(2)}$ in equation (3) consists of 27 elements. However, as the electric field indices j and k can be interchanged for a single beam experiment, the number of independent elements is reduced to 18. After some traditional algebra, the following expression for the SHG intensity can be obtained

$$I(2\omega,t) = \frac{2\mu_0^{3/2}\omega^2 D^2 (\chi_{ijk}^{(2)})^2 I^2(\omega, t-\Delta t)}{\pi \varepsilon_0^{3/2} R^2 n(2\omega) n^2(\omega)} \left[\frac{\sin D\Delta k(t)/2}{D\Delta k(t)/2} \right]^2, \quad (4)$$

where D is the length of the nonlinear medium (i.e., the thickness of the crystal), R the radius of the pumping beam which possesses a Gaussian-like form, μ_0 and ε_0 are the static (low-frequency) values of the magnetic permeability and the electric permittivity, respectively, $n(\omega)$ and $n(2\omega)$ are the refractive indexes for the pumping and the SHG-doubled frequency, respectively, and $\Delta k = k(2\omega) - 2k(\omega)$ is the phase matching wave vector defined by optically induced birefringence. For a centrosymmetric material process, the tensor component $\chi_{ijk}^{(2)}$ is effectively zero because of the symmetry reason, and thus the SHG is forbidden in a centrosymmetric process.

Figure 5 shows the second-order tensor component, where the susceptibility $\chi_{ijk}^{(2)}$, evaluated from the SHG intensities using the relation given in equation (4), is plotted as a function of the thickness of the nanocrystals and copper content. One can see that with decreasing thickness of the crystals, or increasing copper content up to about 0.65%, the value of the tensor component for the SHG significantly increases. As shown earlier,[11] the insertion of the copper impurities favours a stronger local photo-induced anharmonic electron–phonon interaction through the alignment of the local anharmonic dipole moments by the pumping light. As a particular role of the local electron–phonon anharmonicity is described by third-order-rank tensors in disordered systems,[12,18,19] the SHG is very similar to that introduced for the third-

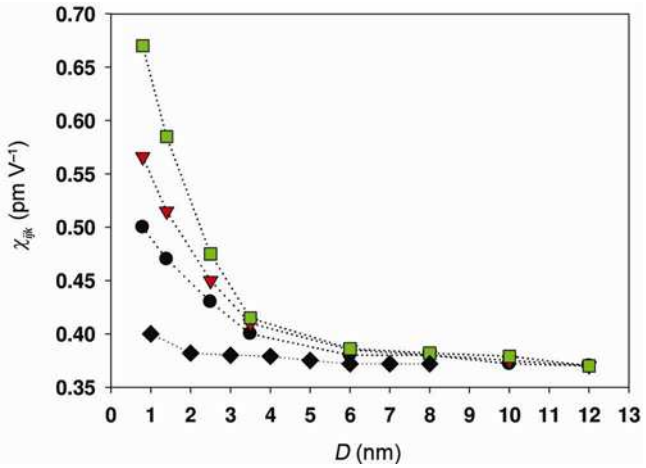

Figure 5. Second-order susceptibility as a function of the size of the nanocrystals for different Cu contents: diamond (1.10%), circle (0.05%), triangle (0.20%) and square (0.65%).

order nonlinear optical susceptibility, which has been confirmed by observing the relatively large third-order susceptibility of undoped CdI_2 single crystals.[7–10]

The local disordering of the copper aggregators plays additional role in the size effect of the nanocrystals.[20–23] As can be seen, for a copper content of about 0.65%, the value of $\chi_{ijk}^{(2)}$ achieves its maximum irrespective of the size of the nanocrystals. Decrease of $\chi_{ijk}^{(2)}$ with a further increase of the copper content might be caused by the aggregation of the copper impurities that is typical of such kinds of layered crystals.[21] The creation of the copper aggregators favours a reduction in the active electron–phonon centres, effectively contributing to the charge density noncentrosymmetry due to copper-induced local electron–phonon anharmonic interaction, as well as leads to the occurrence of metallic clusters,[16] and consequently, suppresses the effect at higher copper content through the limitation of the enhancement of the local hyperpolarizability for the copper aggregators as well as the corresponding nonlinear dielectric susceptibility. However, $\chi_{ijk}^{(2)}$ for a nanocrystal with high copper content was found to be almost equal to that for the undoped crystals, or within the background level.

4. Conclusions

Both pure and Cu-doped CdI_2 nanocrystals were synthesized and grown for the investigation of the SHG. The second-order optical susceptibilities in dependences of the size of the nanocrystals and of their copper contents were calculated. The observed size dependence demonstrates the nanosized quantum-confined effect with a clear increase in the SHG with the decrease in the nanometre size of the crystals. A clear change of the SHG with increase in copper content of the nanocrystals was also observed. The obtained results are discussed on the basis of the electron–phonon anharmonic interaction.

References

1. Haug H (ed.) 1988 *Optical nonlinearities and instabilities in semiconductors* (New York: Academic Press)
2. Born W E (ed.) 1993 *Ultrashort processes in condensed matter* (New York: Plenum Press)
3. Bordas J, Robertson J and Jakobsson A 1978 *J. Phys. C* **11** 2607
4. Robertson J 1979 *J. Phys. C* **12** 4753
5. Dorgii Ya O, Kityk I V, Aleksandrov Yu M, Kolobanov V N, Machov V N and Michailin V V 1985 *J. Appl. Spectrosc.* **43** 1168
6. Catalano I M, Cingolani A, Ferrara R and Lepore M 1985 *Helv. Phys. Acta* **58** 329
7. Miah M I 2002 *Opt. Mater.* **20** 279
8. Miah M I 2004 *Opt. Mater.* **25** 353
9. Miah M I 2009 *Phys. Lett. A* **374** 75
10. Miah M I 2010 *Mater. Chem. Phys.* **119** 402
11. Kityk I V, Pyroha S A, Mydlarz T, Kasperczyk J and Czerwinski M 1998 *Ferroelectrics* **205** 107
12. Bondar V 2000 *Mater. Sci. Eng. B* **70** 258
13. Miah M I 2005 In *The first conference on advances in optical materials*, October 12–15, 2005 (Tucson, Arizona, USA)
14. Herest D and Voolless F 2004 *Opt. Lasers Eng.* **41** 85
15. Miah M I and Kasperczyk J 2009 *Appl. Phys. Lett.* **94** 053117; Miah M I 2011 *Opt. Commun.* **284** 5199
16. Pyroha S A, Metry S, Olekseyuk I D and Kityk I V 2000 *Funct. Mater.* **7** 209
17. Devis C C 1985 *Laser and electro-optics, fundamentals and engineering* (New York: Cambridge University Press)
18. Arun P 2007 *Phys. Lett. A* **364** 157
19. Salimullah M, Shukla P K, Ghosh S K, Nitta H and Hayashi Y 2003 *J. Phys. D* **36** 958
20. McCanny J V, Williams R H, Murray R B and Kemeny P C 1977 *J. Phys. C: Solid State Phys.* **10** 4255
21. Miah M I 2008 *J. Appl. Phys.* **104** 064313
22. Krongman K C, Druffel T and Sunkara M K 2005 *Nanotechnology* **16** 5338
23. Karbovnyk I, Lesivtsiv V, Bolesta I, Velgosh S, Rovetsky I, Pankratov V, Balasubramanian C and Popov A I 2013 *Physica B* **413** 12